JOURNAL OF THERMOPHYSICS AND HEAT TRANSFER
Vol. 9, No. 4, October–December 1995

Near-Isothermal Regenerator: A Perturbation Analysis

Luc Bauwens*
University of Calgary, Calgary, Alberta T2N 1N4, Canada

We develop a perturbation model for regenerators of the type used in Stirling and Gifford–McMahon cryocoolers. The model is valid in the near-isothermal limit, which is usually a quite good approximation for these devices, because typically, the flow passages are small compared to the conductive heat penetration depth in the gas, and because the thermal mass of the heat-storing matrix is large compared to the thermal mass of the gas. Our model is one dimensional and it uses a conventional, empirical model for heat transfer. Our approach can yield solutions for arbitrary heat transfer correlations, which makes it suitable for incorporation in computer models. We also present complete solutions for the important case corresponding to the laminar limit, when the Nusselt number is a constant. Results include the longitudinal temperature distribution and the enthalpy flux through the regenerator. In some conditions, which are more representative of pulse-tube refrigerators than of typical Stirling cryocooler operation, and for which the model remains valid, we obtain multiple solutions, some of which are associated with a sharp temperature peak, in a region in the regenerator where the amplitude of the mass flow rate oscillation exhibits a minimum.

Nomenclature

$A(x)$ = variable defined by Eq. (25)
a = dimensionless parameter characterizing longitudinal conduction, of order unity
b = dimensionless parameter characterizing the matrix thermal mass, of order unity
c_p = specific heat at constant pressure
d = mesh size
I = constant defined by Eq. (27), depends upon the unknown $A(x_2)$
J = constant defined by Eq. (28), depends upon the unknown $A(x_2)$
K = constant defined by Eq. (29), depends upon the unknown $A(x_2)$
k = thermal conductivity
L = length
$\dot{m}$ = mass flow rate
Nu = Nusselt number, based upon mesh size
p = pressure
Q = enthalpy flux through the regenerator
R = gas constant, $c_p - c_v$
Re = Reynolds number
r = ratio of net gas-filled cross section/cross section filled with regenerator material
T = temperature
t = time
x = position
α = heat diffusivity, $k/\rho c_p$
γ = ratio of specific heats, c_p/c_v
ε = small dimensionless number, $d^2/4\alpha\tau$
ρ = density of the cycle fluid
τ = period of revolution

Subscripts

L = corresponding to the left piston and/or heat source
m = refers to the regenerator matrix
R = corresponding to the right piston and/or heat sink
0 = leading-order term in perturbation series
1 = term of order ε in perturbation series
1 = applied to x, refers to the interface left cylinder/regenerator
2 = term of order ε^2 perturbation series
2 = applied to x, refers to the interface regenerator/right cylinder

Received Dec. 9, 1994; revision received March 13, 1995; accepted for publication March 13, 1995.

*Assistant Professor, Department of Mechanical Engineering, 2500 University Drive NW. Member AIAA.

Introduction

THERMAL regenerators are a crucial component in Stirling cryocoolers, particularly at the lower end of the temperature range. This is because, by virtue of the second law, as the temperature ratio becomes large, the heat lifted at the cold end becomes a small fraction of the amplitude of the enthalpy flux oscillation. The regenerator is difficult to analyze because large spatial temperature gradients occur, pressure fluctuates, and both the fluid and the matrix temperature fluctuate while energy is conserved only globally.

On the other hand, if the regenerator is well-designed so that losses are small, the ideal, isothermal Schmidt model[1,2] is a fairly appropriate model for the overall machine. However, by virtue of its ideal nature, the Schmidt model predicts that no loss will occur in the regenerator. To investigate the regenerator losses, we must take into account the smaller, time-dependent temperature fluctuations that the isothermal model neglects.

The classical regenerator model due to Hausen[3] does that, in the context of large recuperators in steel and glass plants, which are open to the atmosphere, and where, as a result, the amplitude of the pressure fluctuations is small compared to the mean pressure. Also, absolute temperature differences are small. Consequently, the incompressible flow assumption is appropriate in these cases. In contrast, Stirling devices are characterized by large absolute temperature ratios between the two ends, and by pressure fluctuations of order unity, with a correspondingly large contribution in the energy equation, which the Hausen model neglects.

We use the more suitable approach originally proposed by Rea and Smith,[4] which is based upon the more appropriate set of assumptions that underlie the isothermal model, but takes them one step further. The isothermal model assumes an infinite matrix thermal mass and an infinite heat transfer coefficient between matrix and gas. In actuality, while both quantities are large, neither is infinite. To take that fact into account, we propose a perturbation analysis, in which both temperatures are modeled as being equal to their isothermal

value, which depends upon position, but is independent of time, plus a small, but time-dependent correction.

If the regenerator were truly isothermal, with a matrix with infinite thermal mass, its temperature would never change from its initial value and any arbitrary initial temperature distribution would be a valid solution. Thus, strictly speaking, the isothermal problem is ill-posed. If the regenerator is not quite isothermal, however, even small time-dependent temperature fluctuations about a mean value will not become periodic functions of time until the mean temperature approaches a spatial distribution such that the net enthalpy flux over one period becomes spatially uniform along the regenerator. One significant implication of the singular nature of the isothermal limit concerns numerical models that directly implement a discretized solution to the nonisothermal conservation equations. These models seek a solution that differs by a small amount from the indeterminate limit, and as a result, the speed at which their solution reaches a periodic limit-cycle approaches zero for data that approach the isothermal limit. This makes them very slow or unreliable, and increasingly so for increasingly better regenerators. In contrast, the approximate perturbation approach that we propose here becomes more accurate for data that approach the isothermal limit, i.e., for very effective regenerators, which are crucial in cryocoolers.

In our model, the time-independent temperature distribution from isothermal analysis corresponds to the "mean" temperature, while the small fluctuations are represented as a perturbation, which results in a small enthalpy flux which, at the stationary regime, becomes uniform. Unbeknownst to us until pointed out by a reviewer, these ideas had originally been proposed in the 1960s by Rea and Smith,[4] and further refined by Qvale and Smith[5] in a context more similar to ours. There is, however, a number of significant differences between our work and theirs. This includes our systematic use of the perturbation formalism, which makes the basic ideas easier to implement and to understand. In our model, the matrix temperature is free to float; they take it to be time-independent. They assume that both pressure and velocities at the regenerator ends vary sinusoidally with respect to time, in effect, linearizing the overall machine; we provide a consistent overall solution that takes the whole machine into account, with no approximation not belonging in the perturbation formalism. While Qvale and Smith[5] do note that the spatial uniformity of the enthalpy flux provides the key condition that determines the temperatures, they did not actually solve for temperatures. Instead, they find an approximate enthalpy flux using an arbitrary temperature distribution that only ensures equality of the flux at both regenerator ends, but not elsewhere. In contrast, we provide a full solution for the temperature profile in the important laminar case. Finally, we present solutions for the whole range of phase angles, and we discuss the interesting phenomena observed for phase angles approaching 180 deg. We show that these are related to pulse-tube refrigeration (which, as Rea and Smith[4] point out, is covered by the analysis) and thermal lag engines.

Significant work in regenerator analysis was performed also, in the 1960s and the 1970s, by Köhler and his co-workers at Philips, who undoubtedly already had the capability to accurately predict regenerator performance. Unfortunately, the reference available in the published literature[6] does not provide enough information to put their work in perspective.

Physical Model

As usual,[7-9] we represent the device as spatially one dimensional. The cycle fluid is an ideal gas with constant specific heats at least locally. In the current model, we neglect pressure gradients, so that the momentum equation plays no further role in the model. (It is clear that however small in relation to the temporal pressure fluctuations, spatial pressure gradients can be very detrimental to performance, so that ultimately, a tradeoff occurs between viscous losses and heat transfer losses. This article concentrates on the latter loss.)

The engine is divided into three volumes: two cylinder spaces and the regenerator. In the cylinders and associated heat exchangers and dead volumes, heat transfer is instantaneous, and the flow is isothermal.

We rescale the longitudinal x coordinate so as to represent volume rather than length. Reynolds numbers and Nusselt numbers are, however, based upon actual areas, velocities, and sizes of the flow passages. This reduces the problem geometry to the simple representation of Fig. 1. The spatial solution domain is the interval $[x_L(t), x_R(t)]$. $x_L(t)$ and $x_R(t)$ describe the piston positions; they are known, periodic, functions of time. The expansion space, including any dead volume between cylinder and heater, is the volume between x_L and x_1. Likewise, the compression space and dead volume are the volume between x_2 and x_R. x_L and x_R vary in time, but x_1 and x_2 are fixed. The regenerator is the volume contained between x_1 and x_2.

Writing heat transfer in terms of an empirical convection model and neglecting the kinetic energy of the fluid, the one-dimensional mass and energy conservation equations for the fluid are

$$\frac{\partial \rho}{\partial t} + \frac{\partial \dot{m}}{\partial x} = 0 \tag{1}$$

$$\rho c_p \frac{\partial T}{\partial t} + c_p \dot{m} \frac{\partial T}{\partial x} - \frac{\mathrm{d}p}{\mathrm{d}t} = \frac{4Nu(Re)k}{d^2}(T_m - T) \tag{2}$$

Both the Nusselt number Nu and the Reynolds number Re are based upon the transverse scale d, which represents the size of the flow passages.

If the Biot number for the matrix mesh is small, then at any given section lengthwise, a lumped mass analysis is appropriate and conservation of energy for the matrix is reduced to Eq. (3), in which r is the ratio of the net cross sections (fluid/matrix)

$$\rho_m c_m \frac{\partial T_m}{\partial t} = k_m \frac{\partial^2 T_m}{\partial x^2} + 4Nu(Re)\frac{rk}{\mathrm{d}^2}(T - T_m) \tag{3}$$

If L is the regenerator length and τ is the period, then, if the residence time of the fluid in the regenerator is of the same order as the period (otherwise the regenerator would probably be very poorly designed anyway), velocities scale with L/τ. Accordingly, Eqs. (4) and (5) are the dimensionless equivalents of our conservation equations, Eqs. (2) and (3), while Eq. (1) is unchanged in dimensionless form:

$$\rho \frac{\partial T}{\partial t} + \dot{m} \frac{\partial T}{\partial x} - \frac{\gamma - 1}{\gamma}\frac{\mathrm{d}p}{\mathrm{d}t} = Nu(Re)\frac{4\alpha\tau}{d^2}(T_m - T) \tag{4}$$

$$\frac{\partial T_m}{\partial t} = \frac{\tau\alpha_m}{L^2}\frac{\partial^2 T_m}{\partial x^2} + Nu(Re)r\frac{\rho c_p}{\rho_m c_m}\frac{4\alpha\tau}{d^2}(T - T_m) \tag{5}$$

Equations (4) and (5) depend upon three dimensionless groups that are normally small in usual designs: $d^2/4\alpha\tau$,

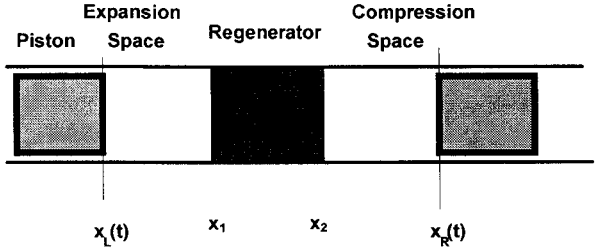

Fig. 1 Notation and indices.

$r\rho c_p/\rho_m c_m$, and $\tau\alpha_m/L^2$. $d^2/4\alpha\tau$ is the inverse of the heat transfer coefficient between gas and matrix, which is large if the amplitude of the temperature oscillation is small; $r\rho c_p/\rho_m c_m$ is the ratio of the thermal mass of the gas by the thermal mass of the matrix; finally, $\tau\alpha_m/L^2$ is a dimensionless longitudinal conduction coefficient.

As for the relative magnitudes of these three small parameters, a large number of situations can arise. We take the first number as our reference, and we write it as ε:

$$\varepsilon = d^2/4\alpha\tau \tag{6}$$

While $r\rho c_p/\rho_m c_m$ is usually very small, it is often not very easy to make ε small, so that the case where $r\rho c_p/\rho_m c_m$ would be larger than ε is unlikely; furthermore, it can easily be avoided and it is not a good design anyway. We concentrate on the case where they are of the same order; to that effect, we introduce the parameter b, which is of order unity:

$$\varepsilon b = r(\rho c_p/\rho_m c_m) \tag{7}$$

Finally, longitudinal conduction is usually very small. It can be verified, and our analysis will confirm that for the effect of the conduction loss not to overwhelm the solution, its maximum magnitude is $\tau\alpha_m/L^2$ of order ε^2. Thus, the constant a defined by Eq. (8) is of order unity. We shall present a complete solution only for a and b of order unity:

$$\varepsilon^2 a = \tau\alpha_m/L^2 \tag{8}$$

Equations (1), (4), and (5), plus the gas laws and the assumption of spatially uniform pressure, provide us with a complete set of equations. Since our analysis focuses upon the regenerator alone, for the remainder of the engine, we adopt the simplest possible assumption: temperatures are fixed and known. That is, the cylinders are isothermal.

The set of approximations described above determines our physical model. Its mathematical equivalent is the following periodic boundary value problem:

The problem is to find time-periodic solutions $\dot{m}(x, t)$, $p(t)$, $\rho(x, t)$, $T(x, t)$ and $T_m(x, t)$, with x defined in the interval $[x_L(t), x_R(t)]$, satisfying Eqs. (9):

$$\frac{\partial\rho}{\partial t} + \frac{\partial\dot{m}}{\partial x} = 0 \tag{9a}$$

$$T = T_L(x) \quad \text{for} \quad x < x_1 \tag{9b}$$

$$\varepsilon\left(\rho\frac{\partial T}{\partial t} + \dot{m}\frac{\partial T}{\partial x} - \frac{\gamma - 1}{\gamma}\frac{dp}{dt}\right) = Nu(Re)(T_m - T) \quad \text{for} \quad x \in (x_1, x_2) \tag{9b'}$$

$$T = T_R(x) \quad \text{for} \quad x > x_2 \tag{9b''}$$

$$\frac{\partial T_m}{\partial t} = \varepsilon^2 a\frac{\partial^2 T_m}{\partial x^2} + bNu(Re)(T - T_m) \quad \text{for} \quad x \in (x_1, x_2) \tag{9c}$$

$$p = \rho T \tag{9d}$$

Boundary conditions are

$$\dot{m}(x_L) = \rho(x_L)\frac{dx_L}{dt} \tag{9e}$$

$$\dot{m}(x_R) = \rho(x_R)\frac{dx_R}{dt} \tag{9f}$$

$x_L(t)$, and $x_R(t)$, the piston positions, are known periodic functions of time with period 1. T_L and T_R are the known heater and cooler wall temperatures. An empirical heat transfer correlation determines the local, instantaneous Nusselt Nu, as a function of the local, instantaneous Reynolds number Re. The total mass of fluid in the machine is equal to 1.

Equation (9a) is the continuity equation, Eq. (1). The cylinders are isothermal, hence, Eqs. (9b) and (9b″). In the regenerator, the energy equation for the fluid is Eq. (9b′). Equation (9c) is the energy equation for the matrix. Equation (9d) is the dimensionless equation of state. At the piston faces, the velocity of the fluid is equal to the piston velocity, providing us with the boundary conditions, Eqs. (9e) and (9f).

Approximate Solution

Perturbation Series

We seek a solution based upon adding a small correction to the simple isothermal solution. This will be most easily done adopting the formal procedure of writing the solution in the form of a perturbation series in ε and solving for a sequence of increasingly smaller corrections. Considering only the regenerator at this point, we write:

$$T = T_0 + \varepsilon T_1 + \varepsilon^2 T_2 + \mathbb{O}(\varepsilon^3) \tag{10a}$$

$$T_m = T_{m0} + \varepsilon T_{m1} + \varepsilon^2 T_{m2} + \mathbb{O}(\varepsilon^3) \tag{10b}$$

$$p = p_0 + \varepsilon p_1 + \varepsilon^2 p_2 + \mathbb{O}(\varepsilon^3) \tag{10c}$$

$$\rho = \rho_0 + \varepsilon\rho_1 + \varepsilon^2\rho_2 + \mathbb{O}(\varepsilon^3) \tag{10d}$$

$$\dot{m} = \dot{m}_0 + \varepsilon\dot{m}_1 + \varepsilon^2\dot{m}_2 + \mathbb{O}(\varepsilon^3) \tag{10e}$$

Replacing the unknowns in Eqs. (9) by their series expressions, Eqs. (10), and setting $\varepsilon = 0$, we obtain the leading-order equations. Then, returning to the complete equations, taking into account that the leading-order problem is now satisfied, so that the terms of order unity now cancel each other, we can divide the equations by ε. Eliminating higher-order terms in the resulting equations, we find the first perturbation problem, etc. Thus, we find a sequence of problems for each of the various orders of accuracy.

Leading-Order Problem

The leading-order problem yields the Schmidt solution, i.e., we find that

$$T_{m0} = T_0 = T_0(x) \tag{11}$$

The continuity equation and the equation of state, applied to the leading-order solution, plus the knowledge about piston motions and the cylinder temperatures, determine the isothermal solution in the usual way. However, all that the isothermal model tells us about temperatures is Eq. (11); i.e., that both temperatures are equal and time-independent, but indeterminate. In the leading-order boundary value problem, the temperatures are merely equal to a space-dependent integration constant. Physically, this is reasonable, because if the thermal mass of the matrix is infinite, no matter what happens, its temperature will never change and it will remain equal at all times to whatever its initial value was.

To find p_0 and $\dot{m}_0$, keeping T_0 as a parameter, we solve the leading-order, isothermal solution, assuming that T_0 is known. To that effect, we integrate leading-order continuity, Eq. (12), which was obtained as the leading-order part of Eq. (9a), between x_L and x, for $x \in (x_1, x_2)$, and we replace density from the state equation $p_0 = \rho_0 T_0$. This results in Eq. (13):

$$\frac{\partial\rho_0}{\partial t} + \frac{\partial}{\partial x}\dot{m}_0 = 0 \tag{12}$$

$$\dot{m}_0 = -\frac{1}{T_L}\frac{d[p_0(x_1 - x_L)]}{dt} - \frac{dp_0}{dt}\int_{x_1}^{x}\frac{1}{T_0}\,dx \tag{13}$$

But integrating Eq. (12) over the whole length of the engine, between x_L and x_R, we have

$$\frac{dp_0}{dt}\left(\frac{x_1 - x_L}{T_L} + \int_{x_1}^{x_2} \frac{1}{T_0}\,dx + \frac{x_R - x_2}{T_R}\right) + p_0\left(\frac{1}{T_R}\frac{dx_R}{dt} - \frac{1}{T_L}\frac{dx_L}{dt}\right) = 0 \tag{14}$$

Equation (14) is an exact integral. Its left-hand side (LHS) equals the time derivative of the total mass of fluid in the machine, which is constant and equal to 1. Integrating, we find the usual equation for pressure from the Schmidt model:

$$p_0 = 1\Big/\left(\frac{x_1 - x_L}{T_L} + \int_{x_1}^{x_2} \frac{1}{T_0}\,dx + \frac{x_R - x_2}{T_R}\right) \tag{15}$$

This does not quite complete the solution because, while an absolute constant, the integral in the denominator of Eq. (15)

$$\int_{x_1}^{x_2} \frac{dx}{T_0}$$

is yet unknown at this stage.

Problem of Order ε

Taking Eq. (11) into account, the components of order ε of Eqs. (9b′) and (9c) are

$$\dot{m}_0 \frac{\partial T_0}{\partial x} - \frac{\gamma - 1}{\gamma}\frac{dp_0}{dt} = Nu(Re_0)(T_{m1} - T_1) \tag{16}$$

$$\frac{\partial T_{m1}}{\partial t} = bNu(Re_0)(T_1 - T_{m1}) \tag{17}$$

If T_0 were known, then p_0 would be fully determined by Eq. (15), and Eqs. (16) and (17) could then be solved for the temperatures T_1 and T_{m1}. However, T_0 remains unknown yet.

Problem of Order ε^2

Adding the $\mathcal{O}(\varepsilon^2)$ perturbation in the energy equation for the fluid, from Eq. (9b′), to the $\mathcal{O}(\varepsilon^2)$ perturbation of the energy equation for the matrix, from Eq. (9c) divided by b, we find

$$\rho_0 \frac{\partial T_1}{\partial t} + \dot{m}_1 \frac{\partial T_0}{\partial x} + \dot{m}_0 \frac{\partial T_1}{\partial x} - \frac{\gamma - 1}{\gamma}\frac{dp_1}{dt} + \frac{1}{b}\frac{\partial T_{m2}}{\partial t} = \frac{a}{b}\frac{\partial^2 T_0}{\partial x^2} \tag{18}$$

Equation (18) includes one new, additional, unknown, T_{m2}. However, in the stationary, periodic regime, T_{m2} is a periodic function of time, and it disappears from the equation obtained by integrating Eq. (18) over one full period of revolution:

$$\frac{d}{dx}\int_0^1 \dot{m}_0 T_1\,dt - \frac{a}{b}\frac{\partial^2 T_0}{\partial x^2} = 0 \tag{19}$$

where we have used the fact that

$$\rho_0 \frac{\partial T_1}{\partial t} = \frac{\partial(\rho_0 T_1)}{\partial t} - T_1 \frac{\partial \rho_0}{\partial t} = \frac{\partial(\rho_0 T_1)}{\partial t} + T_1 \frac{\partial \dot{m}_0}{\partial x}$$

Equation (19) provides a closure to our system of equations. Indeed, we can now solve Eqs. (16) and (17) for T_1 as a function of T_0 and replacing T_1 by that solution in Eq. (19), we obtain an equation in which the only unknown is T_0. Adding b times Eq. (16) to Eq. (17) and integrating with respect to time, we find

$$T_{m1} = b\frac{\gamma - 1}{\gamma}p_0 - b\frac{dT_0}{dx}\int_0^t \dot{m}_0\,dt + C(x) \tag{20}$$

where $C(x)$ is an integration constant. Then, from Eq. (17)

$$T_1 = b\frac{\gamma - 1}{\gamma}p_0 - b\frac{dT_0}{dx}\int_0^t \dot{m}_0\,dt + \frac{1}{Nu(Re_0)}\frac{\gamma - 1}{\gamma}\frac{dp_0}{dt} - \frac{1}{Nu(Re_0)}\frac{dT_0}{dx}\dot{m}_0 + C(x) \tag{21}$$

An equation similar to Eq. (21) was obtained by Qvale and Smith.[5] This is roughly the point where our analysis starts to differ significantly from theirs. In view of their goal to reach a general, but approximate, closed-form expression for ineffectiveness, they continued their analysis in an approximate manner and using a number of empirical inputs. Instead, we proceed with our formal analysis, replacing T_1 from Eq. (21), into Eq. (19), yielding:

$$\frac{d}{dx}\left(b\frac{\gamma - 1}{\gamma}\int_0^1 \dot{m}_0 p_0\,dt + \frac{\gamma - 1}{\gamma}\int_0^1 \frac{\dot{m}_0}{Nu(Re_0)}\frac{dp_0}{dt}\,dt - \frac{dT_0}{dx}\int_0^1 \frac{\dot{m}_0^2}{Nu(Re_0)}\,dt\right) - \frac{a}{b}\frac{d^2T_0}{dx^2} = 0 \tag{22}$$

The first term in the space derivative in Eq. (22) vanishes, because, moving d/dx inside the integral, and taking continuity into account, we can write it as an exact differential. Finally, to find the enthalpy flux, we integrate with respect to x:

$$Q = \frac{\gamma - 1}{\gamma}\int_0^1 \frac{\dot{m}_0}{Nu(Re_0)}\frac{dp_0}{dt}\,dt - \frac{dT_0}{dx}\int_0^1 \frac{\dot{m}_0^2}{Nu(Re_0)}\,dt - \frac{a}{b}\frac{dT_0}{dx} \tag{23}$$

Or, replacing $\dot{m}_0$ by its value from Eq. (13):

$$Q = -\int_0^1 \frac{1}{Nu(Re_0)}\frac{dp_0}{dt}\left\{\frac{1}{T_L}\frac{d[p_0(x_1 - x_L)]}{dt} + \frac{dp_0}{dt}\times\int_{x_1}^{x}\frac{1}{T_0}\,dx\right\}dt - \frac{dT_0}{dx}\int_0^1 \frac{1}{Nu(Re_0)}\left\{\frac{1}{T_L}\frac{d[p_0(x_1 - x_L)]}{dt} + \frac{dp_0}{dt}\int_{x_1}^{x}\frac{1}{T_0}\,dx\right\}^2 dt - \frac{a}{b}\frac{dT_0}{dx} \tag{24}$$

in which p_0 is given by Eq. (15). Equation (24) is an integro-differential equation for T_0. The temperatures T_0 at the two regenerator ends provide boundary conditions to Eq. (24). If the ends of the regenerator matrix are in thermal contact with the cylinder or heat exchanger walls, these temperatures are equal to the temperatures of the cylinder walls. (It can be shown that this is true even without thermal contact. However, that proof is rather long and tedious[9]; we study this issue in detail in an as yet unpublished work.)

Equation (24) is a first-order equation in T_0, with two boundary conditions, $T_0(x_1) = T_L$, and $T_0(x_2) = T_R$, but it also includes the unknown Q. $p_0(t)$, which appears in the time integrals, is given by Eq. (15); it depends upon the yet unknown absolute constant

$$\int_{x_1}^{x_2} \frac{dx}{T_0}$$

Solving

The problem of Eq. (24) can be solved iteratively for arbitrary heat transfer correlations $Nu(Re_0)$, with $Re_0 = \dot{m}d/\rho\nu$. The solution yields the enthalpy flux Q and the temperature profile $T_0(x)$ along the regenerator, resolving the indeterminacy in the relationship between pressures and the mass of fluid in the engine, thus also determining unequivocally the power input and refrigeration.

In the laminar case, Nu is an absolute constant. The laminar case is important as a limit case and it is relevant to low Reynolds number regenerators. Nu being constant, it can then be moved out of the integrals in Eq. (24), which allows us to proceed with a closed-form solution. Taking into account that the integrals of exact differentials of periodic functions over one full cycle vanish, introducing the new unknown $A(x)$, defined by Eq. (25), and the constants I, J, and K, defined by Eqs. (27–29), after some manipulation, Eq. (24) can be transformed into Eq. (26), in which the unknown is $A(x)$:

$$A(x) = \int_{x_1}^{x} \frac{1}{T_0(x)}\,dx \tag{25}$$

$$\frac{d^2A}{dx^2}\frac{1}{\frac{dA}{dx}} = \frac{\gamma - 1}{\gamma}\frac{dA}{dx}\frac{A + I + K}{A^2 + 2IA + J} \tag{26}$$

$$I = \int_0^1 \left\{\frac{d[p_0(x_1 - x_L)]}{dt}\right\}\frac{dp_0}{dt}\,dt \Big/ T_L\int_0^1\left(\frac{dp_0}{dt}\right)^2 dt \tag{27}$$

$$J = \int_0^1 \left\{\frac{[dp_0(x_1 - x_L)]}{dt}\right\}^2 dt + \frac{aNu}{b} \Big/ T_L^2\int_0^1\left(\frac{dp_0}{dt}\right)^2 dt \tag{28}$$

$$K = \frac{\gamma}{\gamma - 1}NuQ \Big/ \int_0^1\left(\frac{dp_0}{dt}\right)^2 dt \tag{29}$$

$p_0(x)$, given by Eq. (15), depends upon $A(x_2)$, which is still unknown. Equation (26) can be integrated between x_1 and x, yielding Eq. (30). Setting $x = x_2$, Eq. (31) is obtained:

$$\frac{T_L}{T_0(x)} = T_L\frac{dA}{dx} = \left(\frac{A^2 + 2IA + J}{J}\right)^{(\gamma-1)/2\gamma}\exp\left[\frac{\gamma - 1}{\gamma} \times \frac{K}{\sqrt{J - I^2}}\left(\arg\tan\frac{A + I}{\sqrt{J - I^2}} - \arg\tan\frac{I}{\sqrt{J - I^2}}\right)\right] \tag{30}$$

$$Q = \frac{\sqrt{J - I^2}}{Nu}\int_0^1\left(\frac{dp_0}{dt}\right)^2 dt \times \frac{\log\frac{T_L}{T_R} - \frac{\gamma - 1}{\gamma}\log\frac{A(x_2)^2 + 2IA(x_2) + J}{J}}{\arg\tan\frac{A(x_2) + I}{\sqrt{J - I^2}} - \arg\tan\frac{I}{\sqrt{J - I^2}}} \tag{31}$$

Equation (31) is an algebraic equation relating the two unknowns Q and $A(x_2)$. Equation (30) is an ordinary differential equation for $A(x)$, which, integrated from x_1 to x_2, would yield another algebraic equation between the same two unknowns Q and $A(x_2)$. Unfortunately, Eq. (30) is not amenable to a closed-form integration, so that, even in the laminar case, the problem still requires a numerical solution.

In this problem, $A(x_2)$ and Q are in effect eigenvalues. Many eigenvalue problems admit multiple solutions, and indeed, we find that in certain conditions, the solution is not unique. It is thus desirable that the numerical solution technique be able to yield multiple solutions. Instead of using the simple Newton iterative method, we scan a reasonable range of tentative values for $A(x_2)$; for each value, we calculate the complete solution, and we identify the intervals over which the difference between calculated $A(x_2)$ and tentative $A(x_2)$ changes sign. This approach provides all the solutions in the scanned range. While more time-consuming than a Newton iteration, it is effective, as the results later show. (Our program is available upon request, for examination and noncommercial use.)

Results

We solved numerically for the laminar, constant Nusselt number case, for two cryocooler configurations, respectively, with a low and a high volume ratio. The same temperature ratio, 1:5 (e.g., 65 K/325 K), was adopted for both configurations. The configuration with low volume ratio corresponds to a typical, not unreasonable cryocooler design, while in the second configuration, the pressure amplitude is much higher than usual. In both cases, displacements were sinusoidal at both ends. In the low amplitude machine, the amplitudes of the piston motion were equal, respectively, to one-tenth of the regenerator volume on the expansion side, and equal to the regenerator volume on the compression side, with dead volumes to midstroke, respectively, equal to 0.2 and 2.4 times the regenerator volumes. In the high-amplitude machine, the piston amplitudes were equal to 0.1 and 2.2 and the dead volumes to midstroke were equal to 0.11 and 2.4 times the regenerator volume. We kept ε and Nu as parameters and we varied the phase angle between piston positions from 0 to 180 deg. For simplicity, conduction losses were assumed to be negligible. (A nonzero value could have been used as easily, but it would have added to the difficulty in analyzing the results.)

Figures 2–4 show, respectively, the eigenvalue $A(x_2)$, the dimensionless gross refrigeration and the dimensionless en-

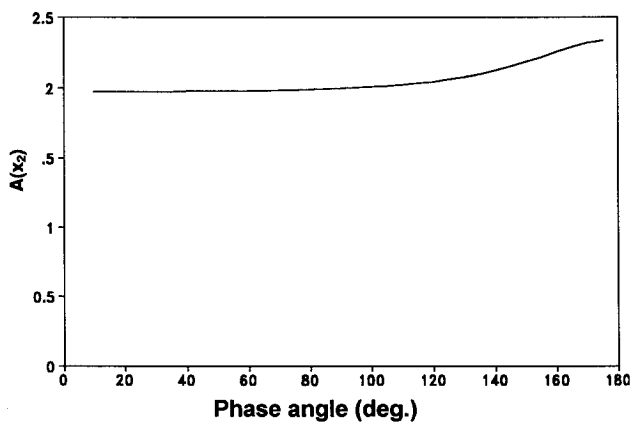

Fig. 2 Eigenvalue $A(x_2)$ vs phase angle; low pressure ratio.

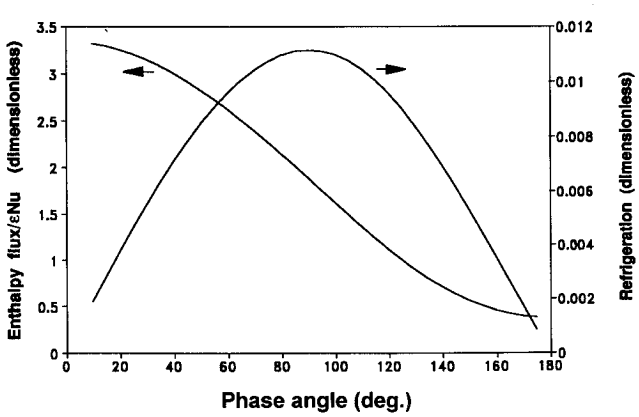

Fig. 3 Enthalpy flux and refrigeration; low pressure ratio.

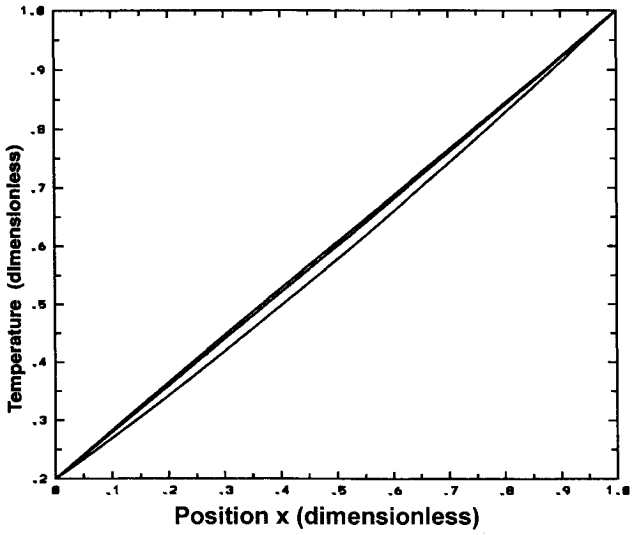

Fig. 4 Temperatures along the regenerator; low pressure ratio; phase angles: 45 deg (upper curve), 90 deg (middle), and 135 deg (lower).

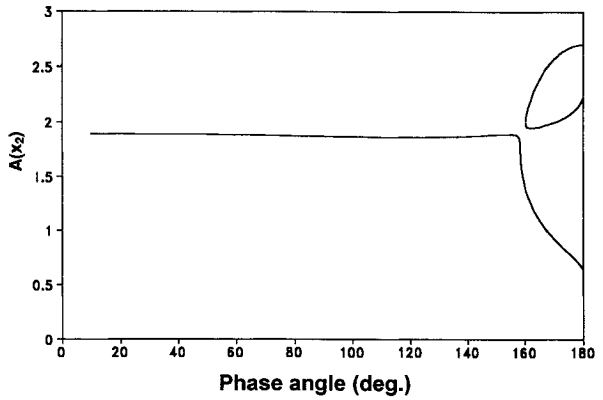

Fig. 5 Eigenvalue $A(x_2)$ vs phase angle; high pressure ratio.

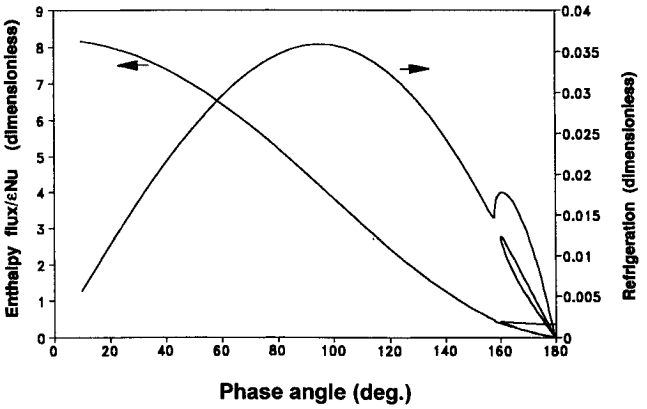

Fig. 6 Enthalpy flux and refrigeration; high pressure ratio.

thalpy flux divided by εNu, and some temperature profiles for the low amplitude machine. Figures 5–12 show similar results for the high amplitude one. These results provide a good example of the power of this analysis and its effectiveness for performance prediction and analysis.

The results show that in both cases, gross refrigeration peaks at a phase angle of approximately 90 deg, as one would expect, while the enthalpy flux decreases monotonically as the phase angle increases, and becomes small for phase angles near 180 deg. We do not present net refrigeration results, because to obtain them, we need to subtract the enthalpy flux from the gross refrigeration, which we could only do for specific values of Nu and $\varepsilon = d^2/4\alpha\tau$. However, since the enthalpy flux decreases monotonically as the phase angle increases, it is clear that the maximum amount of net refrigeration is obtained for a phase angle somewhat higher than 90 deg. This is consistent with the observation that phase angles in a 100–110-deg range are not uncommon in cryocoolers.

While the temperature profiles, on Figs. 4 and 7, clearly depend upon the machine design and operating conditions,

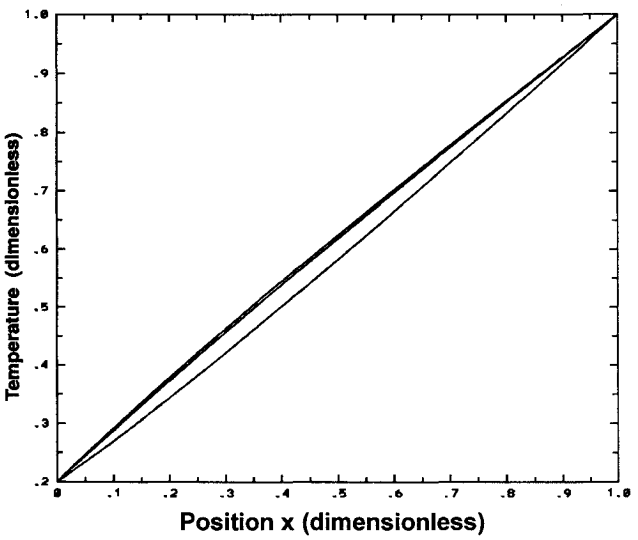

Fig. 7 Temperatures along the regenerator; high pressure ratio; phase angles: 45 deg (lower curve), 90 deg (middle), and 135 deg (upper).

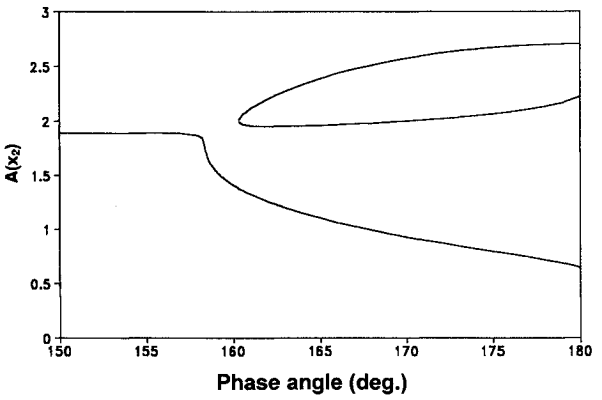

Fig. 8 Eigenvalue $A(x_2)$ for phase angles near 180 deg; high pressure ratio.

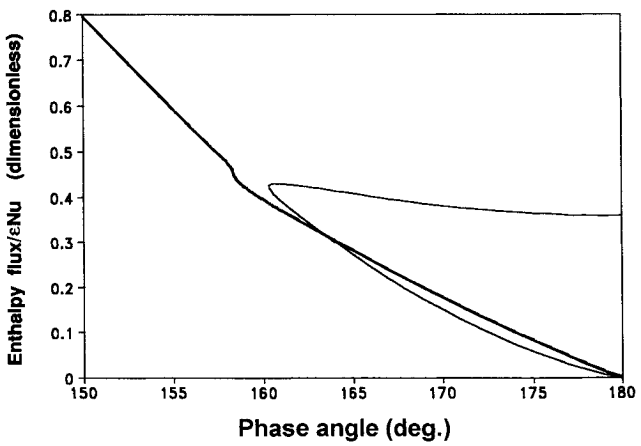

Fig. 9 Enthalpy flux, phase angles near 180 deg; high pressure ratio.

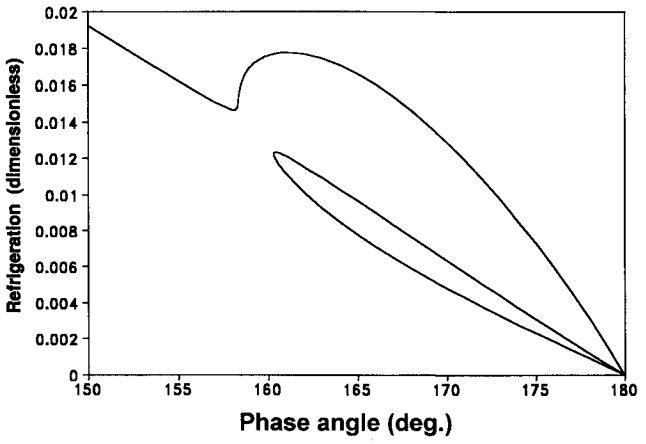

Fig. 10 Refrigeration, phase angles near 180 deg; high pressure ratio.

they do not depart significantly from the linear profile. Since our results were obtained for strictly isothermal cylinders, the temperature of the fluid supplied to the regenerator is fixed, at both ends. Thus, the temperature profiles are not affected by entry effects, which do not appear on the results.

A more surprising phenomenon is observed for the high-amplitude machine, for phase angles approaching 180 deg. Even though this is a very unlikely phase angle for a cryocooler, these results are interesting and they warrant a closer look, for reasons that will become apparent in the analysis below. Figures 8–10 show the same information as Figs. 5 and 6, but are amplified for a small range of phase angles near 180 deg. In order to resolve accurately the behavior in that region, and to make sure that the two curves on Fig. 8 indeed do not intersect as one might expect they would, we investigated the range of phase angles over which the transition occurs using very small intervals, as small as 1/100 of a deg near the nose of the upper branch on Fig. 8.

For values above 164 deg, three solutions exist, corresponding to three different eigenvalues $A(x_2)$. Since our model yields directly the stationary behavior, without mimicking the physical approach process, the existence of multiple solutions does not violate the principle of physical determinacy; indeed, depending upon the initial conditions, the machine may reach a different stationary regime. Furthermore, our technique determines the fixed points regardless of their stability. (If, in some regime, all solutions would reveal to be unstable, inexistence of periodic solutions would raise the specter of possible chaotic solutions.) Further study would require a stability analysis, and an analysis of attraction basins, which would be beyond the scope of this article.

For the smallest of the three eigenvalues $A(x_2)$, Figs. 11 and 12 show a big spike in the temperature profile in the regenerator. That spike can be explained as follows. At 180 deg, both pistons work against each other, in opposite phase. It is easy to verify [e.g., replacing p_0 by its value from Eq. (15) into Eq. (13)] that, in the entire machine, mass flow rates and velocities are then either in phase or in opposite phase with pressure, and that at the interface between these two regions, velocity is always zero, throughout the entire period. In other words, the machine works as if there would be an impenetrable wall at the location of that interface, which for dimensions typical of cryocoolers, with a small expansion space and a large compression space, could either be within the regenerator or in the dead space at the cold end. Knowing $A(x)$, the exact location of that section that the fluid never crosses can easily be calculated. The key difference between the two configurations that we modeled is that in the first case, there is enough dead volume at the expansion end so that the section where velocity is always zero remains within that dead volume, while in the second configuration, for the lowest of the three values of $A(x_2)$, it falls within the regenerator. It is easy to verify that the peak observed in the temperature profile corresponds to that same location within the regenerator.

In effect, in that case, at the phase angle of 180 deg, the machine can be viewed as two half-machines separated by a rigid wall, each of which with one piston periodically compressing the fluid against that wall. Thus, both half-machines work as the pulse-tube in a basic pulse-tube refrigerator (while pulse-tube refrigerators consist of a regenerator and the pulse-tube proper, here we refer to the pulse-tube proper and not the regenerator). But in our model, we have neglected all the mechanisms that would allow heat to flow through the notional wall separating the two halves, or to be removed from the fluid at that location, so that no enthalpy flux can go through, or toward, that wall. This can be checked also in our equations. For a phase angle equal to 180 deg, J equals I^2, and the denominator of the right-hand side (RHS) of Eq. (26) is zero when $A(x) = -I$ (which, by the way, determines the location x of the singularity). The denominator being zero implies that either the enthalpy flux, or dA/dx must be zero, and in the latter case, T_0 goes to infinity at that location. But we show that actually, both conditions are satisfied at the

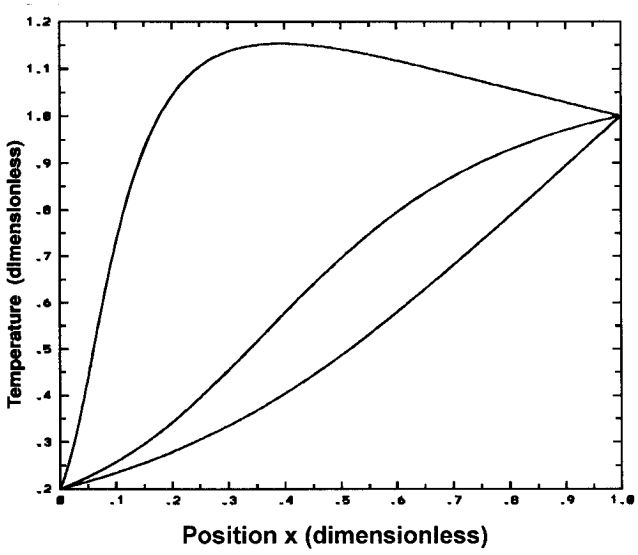

Fig. 11 Temperatures along the regenerator; high pressure ratio; phase angle: 165 deg (all three curves).

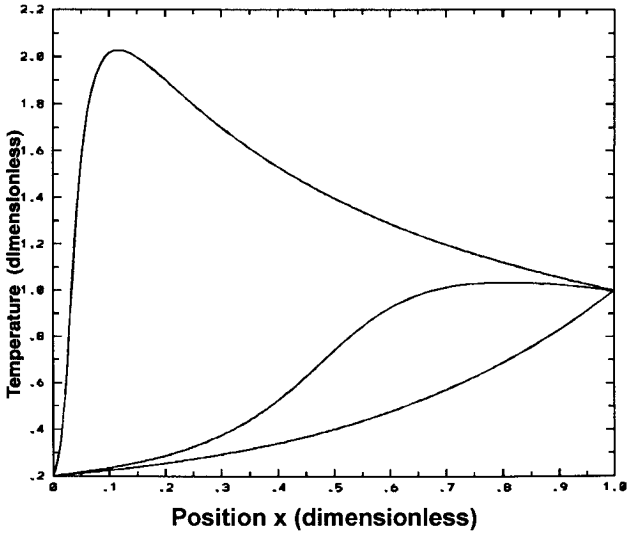

Fig. 12 Temperatures along the regenerator; high pressure ratio; phase angle: 175 deg (all three curves).

singularity. Integration of Eq. (26), respectively, from the left and the right regenerator end, with $J = I^2$, yields

$$\frac{T_0(x)}{T_L} = \left[\frac{I}{A(x) + I}\right]^{(\gamma-1)/\gamma} \exp\left\{-\frac{\gamma - 1}{\gamma}\frac{KA(x)}{I[A(x) + I]}\right\} \tag{32}$$

$$\frac{T_0(x)}{T_R} = \left[\frac{A(x_2) + I}{A(x) + I}\right]^{(\gamma-1)/\gamma} \times \exp\left\{-\frac{\gamma - 1}{\gamma}\frac{K[A(x) - A(x_2)]}{[A(x) + I][A(x_2) + I]}\right\} \tag{33}$$

Both Eqs. (32) and (33) exhibit a singularity at $A = -I$; in both, the first factor goes to infinity while the second, which dominates the limit, approaches either zero for K positive, or infinity for K negative in Eq. (32), and the opposite in Eq. (33). The temperature should approach the same limit coming from either side, which is possible only for K equal to zero, in which case, in both equations, the second factor is unity, while the first factor goes to zero. Thus, K, hence Q, vanishes at the singularity, and, in this case in which we have neglected conduction, both in the wall and in the gas, the temperature goes to infinity. Both half-machines operate as basic pulse-tube refrigerators, but with zero refrigeration because no mechanism has been provided in the model to remove heat at the blind end, where, as a result, temperature has nowhere to go but infinity.

The mechanism that leads to pulse-tube refrigeration according to our model matches the generally accepted pulse-tube refrigeration mechanism.[10] In Eq. (23), the contribution proportional to

$$\int_0^1 \dot{m}_0 \frac{dp_0}{dt}\, dt$$

in the enthalpy flux is a $p\ dV$ term, which is reversible and, with the proper phase relationship between $\dot{m}_0$ and dp_0/dt, is capable of moving heat in the direction opposite the temperature gradient. The other component, however, is proportional to

$$-\frac{dT_0}{dx}\int_0^1 \dot{m}_0^2\, dt$$

which always goes with the temperature gradient.

But our one-dimensional model was developed for matrix topologies much more complex than the straight flow passages typical of pulse tubes, which is why we used an empirical heat transfer model. In an as yet unpublished work, we use the same perturbation technique for two-dimensional, laminar flow in straight passages, with fundamental, diffusive models for heat and momentum. Results show that complete characterization of periodic heat transfer requires two parameters, including the Nusselt number, and an additional parameter, which is different, but which the current analysis based upon the steady flow Nusselt number in effect wrongly assumes to be equal to the Nusselt number. The only impact of that difference is in the exponent of the factor in A^2 on the RHS of Eq. (30) which, for laminar flow in circular tubes, becomes $(4/11)[(\gamma - 1)/\gamma]$ while here, we have $(1/2)[(\gamma - 1)/\gamma]$, but the remainder of the current results is unchanged. Furthermore, in the range of phase angles typical of normal cryocoolers, the numerical impact of this error appears to be very small. In the pulse tube regime, however, results may differ significantly. The bifurcation diagram on Fig. 8 even looks topologically different, albeit still with three solutions for large phase angles. Thus, current results in the pulse tube regime appear to be only qualitatively meaningful.

Conclusions

The proposed perturbation model determines the isothermal temperature profile in the regenerator, thus resolving the indeterminacy of the Schmidt model and allowing for a precise, direct determination of the enthalpy flux, of the regenerator temperature profile, and also, of the relationship between total mass of fluid and mean pressure.

Our model can be implemented numerically for arbitrary heat transfer correlations, which makes it very suitable for incorporation in numerical models of the whole machines, yielding overall results quicker and more reliably than global models that rely upon full discretization, of space and time, and direct numerical solution of the fundamental conservation laws. This is because, in the isothermal limit, the problem that is being solved becomes ill-posed, so that, in the limit, arbitrary regenerator temperature distributions, even discontinuous, become valid solutions. As a result, in contrast with direct numerical solutions of the conservation laws, which become slower and less accurate for more isothermal regenerators, the current approach becomes more accurate. This makes the current approach more trustworthy, much cheaper to implement, and often more accurate.

A complete solution was presented in the laminar limit, for a machine with isothermal cylinders, for phase angles varying between 0–180 deg, showing that the method is effective. Results shown include detailed regenerator temperature profiles; to our knowledge, this is the first time that these profiles were ever calculated, other than numerically.

Finally, for phase angles near 180 deg, these results showed the existence of multiple stationary solutions, due to phenomena akin to pulse tube refrigeration.

References

[1]Schmidt, G., "Theorie der Lehmann'schen kalorische Maschine," *Zeitschrift des Vereins Deutscher Ingenieure*, Vol. 15, No. 1, 1861, pp. 1–9.

[2]Urieli, I., and Berchowitz, D. M., *Stirling Engine Analysis*, Hilger, Bristol, England, UK, 1984.

[3]Hausen, H., "Über die Theorie des Wärmeaustausches in Regeneratoren," *Zeitschrift des Vereins Deutscher Ingenieure*, Vol. 73, 1929, p. 432.

[4]Rea, S. N., and Smith, J. L., Jr., "The Influence of Pressure Cycling on Thermal Regenerators," *Journal of Engineering for Industry, Transactions of the American Society of Mechanical Engineers*, Vol. 89, No. 3, Series B, 1967, pp. 563–569.

[5]Qvale, E. B., and Smith, J. L., Jr. "An Approximate Solution for the Thermal Performance of a Stirling-Engine Regenerator," *Journal of Engineering for Power, Transactions of the American Society of Mechanical Engineers*, Series A, No. 2, 1969, pp. 109–112.

[6]Köhler, J. W. L., Stevens, P. F., de Jonge, A. K., and Beuzekom, D. C., "Computation of Regenerators Used in Regenerative Refrigerators," *Cryogenics*, Vol. 15, No. 9, 1975, pp. 521–530.

[7]Bauwens, L., "A Stratified Flow Model for Adiabatic Losses in Regenerative Thermal Devices," *Emerging Energy Technology -1994-*, edited by G. A. Karim, American Society of Mechanical Engineers, New York, pp. 145–152.

[8]Bauwens, L., "Stirling Cryocooler Model with Stratified Cylinders and Quasisteady Heat Exchangers," *Journal of Thermophysics and Heat Transfer*, Vol. 9, No. 1, 1995, pp. 129–135.

[9]Bauwens, L., "The Near-Isothermal Regenerator: A Perturbation Analysis," *Proceedings of the 29th Intersociety Energy Conversion Engineering Conference*, Vol. 4, AIAA, Washington, DC, pp. 1884–1889, 1994.

[10]De Boer, P. C. T., "Thermodynamic Analysis of the Basic Pulse-Tube Refrigerator," *Cryogenics*, Vol. 34, No. 9, 1994, pp. 699–712.